

## Ground-state correlations in a charged Bose quantum wire

This article has been downloaded from IOPscience. Please scroll down to see the full text article.

1999 J. Phys.: Condens. Matter 11 4665

(<http://iopscience.iop.org/0953-8984/11/24/308>)

View [the table of contents for this issue](#), or go to the [journal homepage](#) for more

Download details:

IP Address: 171.66.16.214

The article was downloaded on 15/05/2010 at 11:49

Please note that [terms and conditions apply](#).

## Ground-state correlations in a charged Bose quantum wire

R K Moudgil†‡, K Tankeshwar§ and K N Pathak§

† School of Basic and Applied Sciences, Thapar Institute of Engineering and Technology, Patiala-147 001, India

‡ Department of Physics, Kurukshetra University, Kurukshetra-136 119, India

§ Department of Physics, Panjab University, Chandigarh-160 014, India

Received 7 July 1998

**Abstract.** We study the ground-state correlations in a charged Bose quantum wire within the self-consistent-field approximation of Singwi, Tosi, Land, and Sjölander. A simple cylindrical model for the quantum wire is used. Static properties (structure factor, pair correlation function, and screened interaction potential), elementary excitation spectra, and ground-state energies are calculated at different boson number densities and wire radii. Our study shows that, in addition to the density of bosons, the wire radius provides an extra control on the strength of the many-body correlations. The correlation effects are found to become increasingly important with decreasing wire radius at a fixed density, and vice versa. The results obtained using the lower-order random-phase approximation are also given. We have compared our results for the screened potential with those for the semiconductor electron quantum wire. It is found that the screened potential for charged bosons is more attractive than that for electrons for  $r_s < 8$ , while the two potentials become essentially the same for  $r_s > 8$ . Therefore, we conclude that the exchange effects associated with the electron statistics act to oppose the overscreening properties of the charged Bose system and are dominated by the Coulomb correlation effects at low carrier densities corresponding to  $r_s > 8$ .

### 1. Introduction

The study of a system of charged point-like bosons embedded in a uniform neutralizing background has attracted considerable interest in the recent years. This arises mainly from their importance in exploring the role of particle statistics in the many-body correlations and partly from their recognition as a possible model for understanding the phenomenon of high-temperature superconductivity [1, 2]. A comparison between the behaviour of charged Bose and electron fluids is anticipated to yield information about the contributions of exchange and Coulomb effects to correlations. At present, a reasonable amount of information is available regarding the ground-state correlations in three-dimensional (3D) [3, 4] and two-dimensional (2D) [4, 5] charged Bose systems due to the combined efforts of theoretical studies and quantum Monte Carlo simulation experiments. The study of correlations has also been extended to the double- and multi-layer charged Bose systems [6].

Recently, Gold [7] has suggested that the system of charged Bose multiple quantum wires might be a useful model for understanding superconductivity in the one-dimensional (1D) structures (organic superconductors [8]). Therefore, presumably, an understanding of many-body correlations in 1D may have importance in the context of the theory of 1D superconductors. These correlations have been extensively studied in the 1D electron systems (the so-called electron quantum wires) both theoretically [9] and experimentally [10]. However, similar studies are lacking for 1D charged Bose systems. Experimental study of the charged

Bose system (not only in 1D, but also in the higher dimensions) has not yet been possible because these systems, unlike their electron counterparts, have not so far been realized in the laboratory. Theoretically, Gold [7] has presented some preliminary results for the elementary excitation spectrum of the charged Bose multiple-quantum-wire system on the basis of the random-phase approximation (RPA). However, the RPA completely neglects the short-range correlations between the charged bosons which are in fact known to become even more important in reduced dimensions. Thus, these effects, when taken into consideration, are expected to modify the excitation spectrum. In the present work, we investigate the many-body correlations in an isolated charged Bose quantum wire beyond the RPA. A simple cylindrical model proposed by Gold and Ghazali [11] is used, where an analytical expression for the Coulomb interaction potential between bosons has been developed in the Fourier space. Correlations beyond the RPA are described within the self-consistent-field approximation of Singwi, Tosi, Land, and Sjölander (STLS) [12]. The STLS theory includes correlations in the form of a static local field correction to the bare interaction between bosons, and the correction factor is to be obtained numerically in a self-consistent way. It is worthwhile to mention here that the STLS theory was originally developed for the electron gas system, and has been applied in the study of ground-state behaviour of charged Bose systems in 3D [13] and 2D [5]. On including the local field correction, the excitation spectrum can be calculated at different boson number densities. We also present results for the static structure factor, pair correlation function, static screened potential, and ground-state energy. In the cylindrical wire model, the wire radius appears directly in the Coulomb interaction potential, and is therefore expected to influence the contribution of many-body correlations. Motivated by the above considerations, we have investigated in a systematic way the correlations at different wire radii. The screened potential is discussed in comparison with the results for electron quantum wires. The comparison may be helpful for disentangling the exchange and Coulomb contributions to the correlations.

The paper is organized as follows. In section 2, we describe the quantum wire model and the theoretical formalism. Results and a discussion are given in section 3. A summary and the conclusions are presented in section 4.

## 2. Wire model and theory

### 2.1. Wire model

We consider a system of charged point-like particles of charge  $e$  each obeying the Bose–Einstein statistics and confined to moving freely along one spatial direction (say, the  $x$ -axis), while their motion is restricted to being along the two transverse directions. The model is a direct Bose analogue of the quasi-one-dimensional (Q1D) electron system. The Q1D electron system realized in the laboratory has been modelled theoretically using different geometrical constraints. However, the qualitative behaviour of correlations is found to be more or less the same irrespective of the wire geometry. We use in the present work the cylindrical quantum wire model developed in the context of an electron system by Gold and Ghazali [11]. In this model, the Q1D structure is a circular cylinder of radius  $R_0$  with an infinite potential barrier at  $r = R_0$ . The motion of the carriers is free along the cylinder axis, while it is restricted perpendicular to the cylinder. At absolute zero temperature, the bosons are assumed to be present in the condensate state. This assumption results in a simplification of the problem as compared to the corresponding one for the electron wire where the electrons can occupy the higher-energy subbands in the transverse direction. The wire system is assumed to be embedded in a uniform neutralizing background. For the Coulomb interaction potential between bosons, we use the

analytical result developed by Gold and Ghazali. The potential is given as

$$V(q) = \frac{e^2}{2\epsilon_0} f(q) \quad (1)$$

where

$$f(q) = \frac{144}{(qR_0)^2} \left[ \frac{1}{10} - \frac{2}{3(qR_0)^2} + \frac{32}{3(qR_0)^4} - 64 \frac{I_3(qR_0)K_3(qR_0)}{(qR_0)^4} \right]. \quad (2)$$

$I_n(x)$  and  $K_n(x)$  are the modified Bessel functions of order  $n$ .  $\epsilon_0$  is the dielectric constant of the background, and we will use  $\epsilon_0 = 1$ . In the long-wavelength limit,  $V(q)$  exhibits logarithmic divergence, i.e.,  $V(q) \approx \ln(qR_0)$  as  $q$  approaches zero, and this behaviour is also found in the other Q1D models.

## 2.2. Theory

The dielectric formulation offers a simple and compact way of describing the physical behaviour of the many-body charged systems. The density response function  $\chi(q, \omega)$ , which represents the density response of the system to an external electric potential of wave vector  $q$  and frequency  $\omega$ , is a quantity of central importance, as it contains all of the relevant information about the system.  $q$  is the 1D wave vector along the cylinder axis. An exact calculation of  $\chi(q, \omega)$  is not practically feasible, as it amounts to solving the complicated many-body problem. Within the mean-field approximation,  $\chi(q, \omega)$  is given by

$$\chi(q, \omega) = \frac{\chi_0(q, \omega)}{1 - V(q)[1 - G(q)]\chi_0(q, \omega)}. \quad (3)$$

$\chi_0(q, \omega)$  is the response function for the noninteracting charged Bose system, and at absolute zero temperature it is given by

$$\chi_0(q, \omega) = \frac{2n\epsilon_q}{\omega^2 - \epsilon_q^2} \quad (4)$$

where  $\epsilon_q = (\hbar q)^2/(2m)$  is the free-particle energy, and  $n$  denotes the linear density of bosons. It may be noted that  $\chi_0(q, \omega)$  has the same analytical expression independently of the dimensionality.  $G(q)$  appearing in equation (3) is the local field correction arising due to short-range correlations between the charged bosons. We employ the theory of Singwi *et al* (STLS) for calculating  $G(q)$ , and it is given by

$$G(q) = -\frac{1}{n} \int_{-\infty}^{\infty} \frac{dq'}{2\pi} \frac{q'V(q')}{qV(q)} [S(q - q') - 1]. \quad (5)$$

$S(q)$  is the static structure factor which is related to the imaginary part,  $\chi''(q, \omega)$ , of  $\chi(q, \omega)$  through the fluctuation-dissipation theorem as follows:

$$S(q) = -\frac{\hbar}{\pi n} \int_0^{\infty} d\omega \chi''(q, \omega). \quad (6)$$

The  $\omega$ -integration can be performed analytically to give  $S(q)$  as

$$S(q) = \left[ 1 + \frac{2nV(q)(1 - G(q))}{\epsilon_q} \right]^{1/2}. \quad (7)$$

From equations (5) and (7), it is apparent that  $G(q)$  can be obtained numerically in a self-consistent way. From the calculation of  $G(q)$ , and hence  $\chi(q, \omega)$ , we deduce in the next section various static and dynamic properties of the system.

### 3. Results and discussion

For the numerical calculations and the results presented (unless stated otherwise) we choose a system of units in which  $\hbar = 1$  and the lengths and energies are expressed, respectively, in units of the Bohr atomic radius ( $a_0$ ) and the rydberg ( $1 \text{ Ryd} = e^2/(2a_0)$ ). The density of bosons is described by a dimensionless parameter  $r_s$ :  $r_s = 1/(2na_0)$ .

#### 3.1. Static correlation functions

Expressed in dimensionless units,  $S(q)$  and  $G(q)$  become

$$S(q) = \left[ 1 + \frac{f(q)}{r_s q^2} (1 - G(q)) \right]^{-1/2} \quad (8)$$

$$G(q) = -\frac{r_s}{\pi q f(q)} \int_0^\infty dq' [S(q') - 1] [(q + q')f(q + q') + (q - q')f(q - q')]. \quad (9)$$

Equations (8) and (9) are solved numerically in a self-consistent way by taking the RPA ( $G(q) = 0$ ) structure factor as the initial guess for calculating  $S(q)$  and  $G(q)$ . A self-consistent solution is obtained within a tolerance of 0.01% in about 10–20 iterations, depending upon the value of  $r_s$  and the wire radius  $R_0$ . The results for the self-consistent structure factor  $S(q)$  and local field correction  $G(q)$  are plotted in figures 1 and 2 for  $r_s = 1, 3, 5, 8$  and  $R_0 = 2$ . The behaviour of  $G(q)$  implies an increase in the local field correction due to many-body correlations with increasing  $r_s$ , i.e. decreasing density of bosons. We find a similar qualitative behaviour of  $G(q)$  with decreasing wire radius  $R_0$  at a fixed density  $r_s$ . This result will be illustrated more transparently in the real space while discussing the pair correlation function and the screened potential. We find the following limiting behaviours of  $S(q)$  and  $G(q)$ :

$$\lim_{q \rightarrow 0} S(q) \approx 2q \sqrt{\frac{r_s}{|\ln(q R_0/2)|}} \quad (10)$$

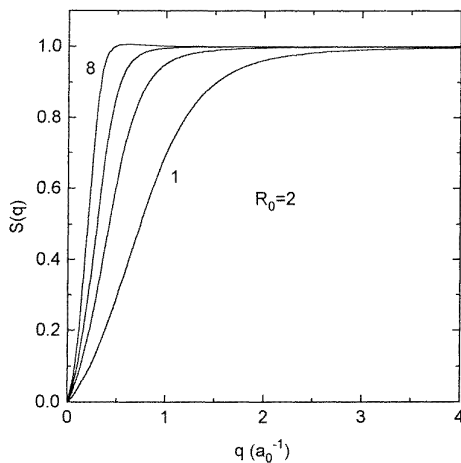


**Figure 1.** The static structure factor  $S(q)$  versus  $q$  for  $r_s = 1, 3, 5, 8$  and  $R_0 = 2$ . The curves from bottom to top represent  $S(q)$  in increasing order of  $r_s$ .

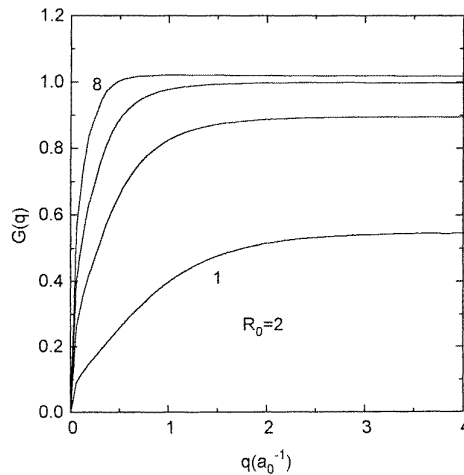


**Figure 2.** The local field correction  $G(q)$  versus  $q$  for  $r_s = 1, 3, 5, 8$  and  $R_0 = 2$ . The curves from bottom to top represent  $G(q)$  in increasing order of  $r_s$ .

and

$$\lim_{q \rightarrow 0} G(q) \approx -\frac{r_s \gamma}{\pi \ln(q R_0/2)} \left[ 1 - \frac{1}{8} (q R_0)^2 \right] \quad (11)$$

$$\lim_{q \rightarrow \infty} G(q) \approx 1 - g(0) \quad (12)$$

where

$$\gamma = -\frac{1}{2} \int_0^\infty dq f(q) [S(q) - 1] \quad (13)$$

is a positive-definite quantity and  $g(0)$  is the value of the pair correlation function at zero separation. The large- $q$  result is identical with that obtained for the 2D and 3D systems, while the small- $q$  behaviour is different and depends strongly on the wire size. Relation (11) shows that the effect of increasing  $r_s$  can be achieved equivalently by decreasing the value of  $R_0$ . We find numerically that this is true for all values of  $q$ . A similar behaviour of  $G(q)$  holds for the electron quantum wire [14]. This result could be of use in fabricating the strongly correlated electron system in semiconductor heterojunctions even at moderately high electron densities by adjusting the width of the confining potential.

The pair correlation function  $g(x)$  can be obtained from  $S(q)$  by taking its inverse Fourier transform as follows:

$$g(x) = 1 + \frac{2r_s}{\pi} \int_0^\infty dq \cos(qx) [S(q) - 1]. \quad (14)$$

$S(q)$  calculated self-consistently is used in the above equation to calculate  $g(x)$ , and the results thus obtained are plotted in figure 3(a) as solid curves for different  $r_s$  at a fixed wire radius  $R_0 = 2$ . The dashed curves in figure 3(a) represent  $g(x)$  in the RPA for  $r_s = 1$  and 3. In the RPA,  $g(x)$  is found to become negative at small separation for  $r_s \geq 2$ . It is the inclusion of short-range correlations in the form of a local field correction that repairs this unphysical behaviour of  $g(x)$ , and  $g(x)$  in STLS theory becomes only slightly negative for  $r_s \geq 8$ . Now,

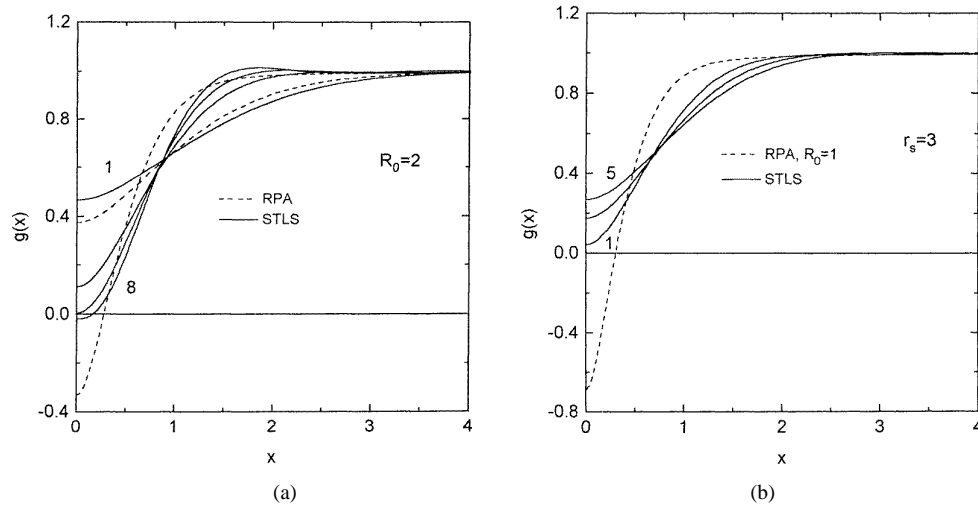


**Figure 3.** The pair correlation function  $g(x)$  versus  $x$  for (a)  $r_s = 1, 3, 5, 8$  and  $R_0 = 2$ ; the curves in the order of decreasing  $g(0)$  represent  $g(x)$  in increasing order of  $r_s$ , and (b)  $R_0 = 1, 3, 5$  and  $r_s = 3$ ; the curves in the order of decreasing  $g(0)$  represent  $g(x)$  in decreasing order of  $R_0$ .  $x$  is in units of  $(\pi/(4r_s a_0))^{-1}$ . The solid curves are the results from STLS theory, and the dashed curves represent the RPA results.

we study  $g(x)$  as a function of the wire radius, keeping  $r_s$  fixed. In figure 3(b),  $g(x)$  is shown for  $R_0 = 1, 3, 5$  and  $r_s = 3$  along with the RPA result (dashed curve) for  $R_0 = 1$ . Making a comparison between the results for  $g(x)$  in figures 3(a) and 3(b), we find that, in addition to the density of bosons, the wire width provides an extra control on the strength of the many-body correlations. For a fixed density, the correlations are found to grow in magnitude with decreasing wire radius and vice versa. The importance of correlations with decreasing  $R_0$  is also apparent in the behaviour of  $g(x)$  in the RPA. For example, the RPA estimate of  $g(0)$  decreases from  $-0.332$  ( $R_0 = 2$ ) to  $-0.686$  ( $R_0 = 1$ ) at  $r_s = 3$  (figure 3).

### 3.2. Static screened potential

The static screened interaction potential  $V_{sc}(q)$  is defined by

$$V_{sc}(q) = \frac{V(q)}{\epsilon(q, \omega = 0)} \quad (15)$$

where  $\epsilon(q, \omega = 0)$  is the static dielectric response function, which in STLS theory is given by

$$\frac{1}{\epsilon(q, \omega = 0)} = 1 + V(q)\chi(q, \omega = 0). \quad (16)$$

In real space the screened Coulomb interaction potential  $V_{sc}(x)$  is given by inverse Fourier transformation as

$$V_{sc}(x) = \frac{1}{\pi} \int_0^\infty dq \cos(qx) V_{sc}(q). \quad (17)$$

In figure 4(a) we show the screened potential  $V_{sc}(x)$  versus distance  $x$  for  $r_s = 1, 3, 5, 8$  and  $R_0 = 2$  along with the RPA results (dashed curves) for  $r_s = 1$  and 5. The dash-dot curve is for the unscreened Coulomb potential for  $r_s = 1$  and  $R_0 = 2$ . It must be pointed out here that the interaction potential  $V(q)$  has been calculated by averaging over the Schrödinger

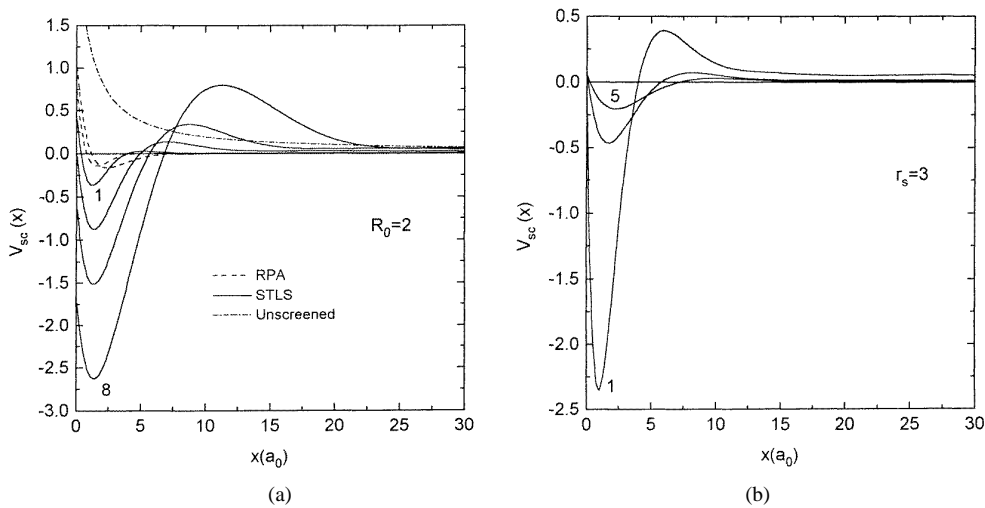


**Figure 4.** The static screened potential  $V_{sc}(x)$  versus  $x$  for the Bose system for (a)  $r_s = 1, 3, 5, 8$  and  $R_0 = 2$ ; the curves from top to bottom represent  $V_{sc}(x)$  in increasing order of  $r_s$ , and (b)  $R_0 = 1, 3, 5$  and  $r_s = 3$ ; the curves from top to bottom represent  $V_{sc}(x)$  in decreasing order of  $R_0$ . The solid curves are the results from STLS theory and the dashed and dash-dot curves represent, respectively, the RPA results and the unscreened potential.

wave functions corresponding to the geometry of the cylinder. Thus,  $x$  represents the parallel separation between two particles. The finite  $V(x)$  at  $x = 0$  is due to averaging effects. From figure 4(a), we find that  $V_{sc}(x)$  exhibits an attractive region, and its depth is strongly enhanced over the RPA value by the many-body correlations. Also, the many-body enhancement of the attraction increases with the decrease in density. The comparison with the RPA curves shows that  $V_{sc}(x)$  is already negative in the RPA. We also check that the attraction continues to appear in  $V_{sc}(x)$  even in the high-density limit, i.e., for  $r_s \ll 1$ . This behaviour of the charged Bose fluid is well known in higher dimensions and is called overscreening. We may conclude from the comparison that the correlations between bosons further enhance the overscreening properties. In order to illustrate the dependence of the correlations on the wire radius,  $V_{sc}(x)$  is plotted in figure 4(b) for different wire radii ( $R_0 = 1, 3, 5$ ) and a fixed density ( $r_s = 3$ ). Clearly, the correlations build in strength with decreasing  $R_0$ . The correlations at  $r_s = 8$  and  $R_0 = 2$  seem approximately identical with those at  $r_s = 3$  and  $R_0 = 1$ .

It is interesting to compare our results for the screened potential with the electron quantum wire system. The comparison is presented in figure 5 for  $r_s = 1, 3, 8$  and  $R_0 = 2$ . The solid and dashed curves represent, respectively, the results for the charged Bose and electron wires.  $V_{sc}(x)$  for the electron system is qualitatively the same as for the Bose case except for the presence of oscillatory behaviour in the former at large  $r$ . These oscillations (Friedel oscillations) are present due to the singular behaviour of the 1D Lindhard function at  $q = 2q_F$ ,  $q_F$  being the Fermi wave vector. The difference in results for  $V_{sc}(x)$  is certainly due to the different statistics obeyed by the particles in the two systems. At  $r_s = 1$ ,  $V_{sc}(x)$  for the Fermi case is negligibly attractive as compared to that for the Bose case, and the two curves differ considerably. With increasing  $r_s$ , however, the difference in results becomes smaller, and for  $r_s \geq 8$ , the potentials  $V_{sc}(x)$  are hardly distinguishable for the two systems. Thus, we may conclude from the comparative study that the exchange effects make the dominant contribution to the many-body correlations in the high-density regime, and that the Coulomb effects grow with decreasing density and eventually dominate over exchange effects in the low-density regime. A similar relative importance of exchange and Coulomb correlations as a function of  $r_s$  is also seen in the behaviour of  $g(x)$ . Furthermore, the above comparison suggests that the exchange effects associated with the Fermi statistics oppose the overscreening nature of

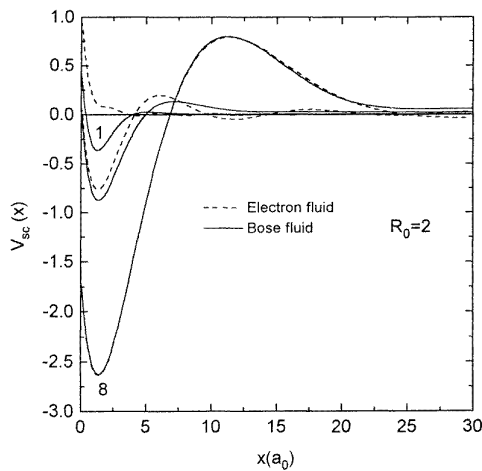


**Figure 5.** The static screened potential  $V_{sc}(x)$  versus  $x$  for  $r_s = 1, 3, 8$  and  $R_0 = 2$ ; the solid and the dashed curves represent, respectively,  $V_{sc}(x)$  for the Bose and the Fermi cases.



the Bose statistics. However, the Coulomb correlations grow more quickly than the exchange effects with increasing  $r_s$ , and consequently one expects overscreening effects in the electron gas as well, but at sufficiently large  $r_s$ . Calmels and Gold [14] have also recently anticipated the presence of overscreening effects in the electron wire at large  $r_s$ . Our study, however, provides a clear quantitative basis for the anti-overscreening nature of exchange effects at small  $r_s$  and for the dominance of Coulomb correlations, and, hence, overscreening at high  $r_s$ .

### 3.3. The elementary excitation spectrum

The spectrum of elementary excitations is obtained from the poles of the density response function, i.e.,

$$1 - V(q)[1 - G(q)]\chi_0(q, \omega_p(q)) = 0. \quad (18)$$

Solving equation (18), we obtain  $E(q)$  ( $= \hbar\omega_p(q)$ ) as

$$E(q) = \left[ q^4 + \frac{q^2 f(q)}{r_s} (1 - G(q)) \right]^{1/2}. \quad (19)$$

In the long-wavelength limit,  $E(q)$  is given approximately by

$$E(q) \approx \frac{2q}{\sqrt{r_s}} |\ln(qR_0/2)|^{1/2} \left[ 1 + \frac{r_s \gamma}{2\pi \ln(qR_0/2)} \right] \quad (20)$$

and in the large- $q$  limit,  $E(q)$  asymptotically approaches the free-particle energy.  $E(q)$  represents the energy of the collective excitation of bosons (plasmons) along the length of the cylinder. Figures 6(a) and 6(b) show, respectively, the results for  $E(q)$  for  $r_s = 1, 3, 5, 8$ ;  $R_0 = 2$  and  $R_0 = 1, 3, 5$ ;  $r_s = 3$ . The results obtained using the RPA are also plotted for comparison, as dashed curves. Again we notice that the difference in results from STLS theory and the RPA is maximum for low densities and smaller wire radii, where correlations play a more important role.

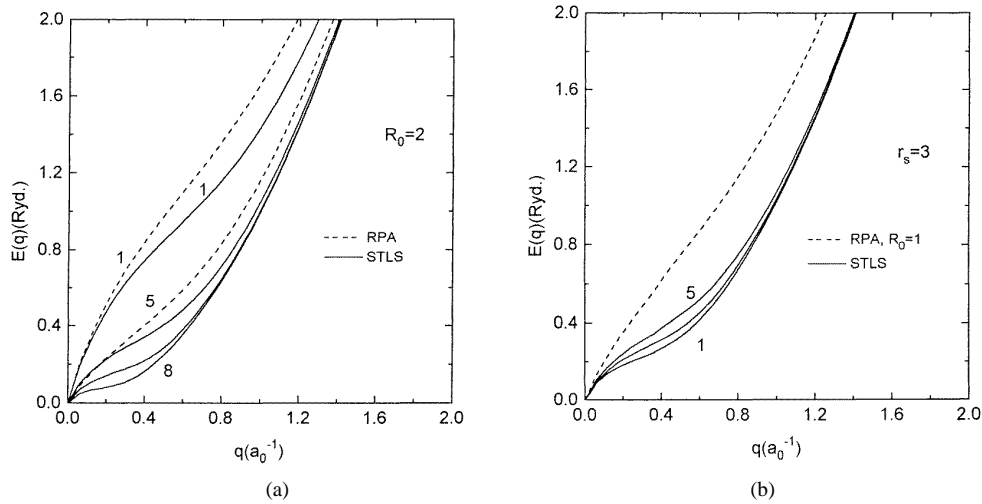


**Figure 6.** The excitation energy  $E(q)$  versus  $q$  for (a)  $r_s = 1, 3, 5, 8$  and  $R_0 = 2$ ; the curves from top to bottom represent  $E(q)$  in increasing order of  $r_s$ , and (b)  $R_0 = 1, 3, 5$  and  $r_s = 3$ ; the curves from top to bottom represent  $E(q)$  in decreasing order of  $R_0$ . The solid curves are the results from STLS theory and the dashed curves represent the RPA results.

### 3.4. Ground-state energy

The ground-state energy  $E_{gs}$  is simply equal to the boson interaction energy ( $E_{int}$ ), as the kinetic energy contribution is zero in the condensate phase.  $E_{int}$  is determined by using the ground-state energy theorem as

$$E_{int} = \int_0^{e^2} d\lambda \frac{E_{int}(\lambda)}{\lambda} \quad (21)$$

where  $\lambda$  measures the strength of the interaction potential and  $E_{int}(\lambda)$  is given by

$$E_{int}(e^2) = \frac{n}{2N} \sum_q V(q)[S(q) - 1]. \quad (22)$$

From equations (21) and (22),  $E_{gs}$  (in rydbergs) is obtained as

$$E_{gs} = \frac{1}{2\pi r_s} \int_0^{r_s} dr'_s \int_0^\infty dq f(q)[S(q; r'_s) - 1]. \quad (23)$$

Equation (23) is solved numerically to calculate  $E_{gs}$  and the results are given in table 1 as a function of  $r_s$  for  $R_0 = 2$ , along with the RPA values. Correlation effects are clearly overestimated in the RPA.

**Table 1.** The ground-state energy ( $-E_{gs}$  in rydbergs) as a function of  $r_s$  for  $R_0 = 2$ .

$r_s$	1	2	3	5	8
STLS	0.3496	0.3113	0.2850	0.2465	0.2059
RPA	0.3612	0.3328	0.3156	0.2934	0.2717

## 4. Summary and conclusions

We have studied the ground-state correlations in a charged Bose quantum wire beyond the random-phase approximation by including the correction due to many-body correlations. Correlation effects are described within the self-consistent-field approximation of Singwi, Tosi, Land, and Sjölander. Static pair correlation functions, static screened interaction potentials, elementary excitation spectra, and ground-state energies are calculated, and their dependence on the boson number density and the wire radius is examined. The comparison with the RPA shows that the correlations beyond the RPA become increasingly important with (i) decreasing density of bosons and (ii) decreasing wire radius. We have also presented a comparison between the results for charged Bose and electron wires in terms of the static screened potential. The comparison makes it clear that the exchange effects of Fermi statistics work against the overscreening property of the charged Bose system, while the Coulomb correlations support the overscreening. Overscreening enhanced by many-body correlations may provide a mechanism for the formation of bound pairs of electrons (local pairing [2]). If this happens, the paired-electron system constitutes a system of charged bosons with a density about half that for the unpaired-electron system. Consequently, one should expect the formation of bound pairs of bosons due to overscreening. This seems possible as long as the charged bosons are point-like particles. However, the bound pairs of electrons have a finite size, and we believe that their screening behaviour will be different from that of point-like charged bosons—because, if this is not true, the system of point-like charged bosons will become unstable against local pairing. Therefore, it will be important to study the ground-state correlations considering the finite size of the bosons. Furthermore, it is hoped that our study will stimulate work on the problem—in

particular, the computer simulation of the ground-state properties of quasi-one-dimensional systems of charged bosons and electrons.

## References

- [1] Mott N F 1987 *Nature* **327** 185  
Alexandrov A S and Mott N F 1993 *Phys. Rev. Lett.* **71** 1075  
Alexandrov A S, Beere W H, Kabonov V V and Liang W Y 1997 *Phys. Rev. Lett.* **79** 1551
- [2] Micnas R, Ranninger J and Robaszkiewicz S 1990 *Rev. Mod. Phys.* **62** 113
- [3] Conti S, Chiofalo M L and Tosi M P 1994 *J. Phys.: Condens. Matter* **6** 8795  
Moroni S, Conti S and Tosi M P 1996 *Phys. Rev. B* **53** 9688 and references therein
- [4] Apaja V, Halinen J, Halonen V, Krotscheck E and Saarela M 1997 *Phys. Rev. B* **55** 12 925 and references therein
- [5] Moudgil R K, Ahluwalia P K, Tankeshwar K and Pathak K N 1997 *Phys. Rev. B* **55** 544 and references therein  
Alder B J and Peters D S 1989 *Europhys. Lett.* **10** 1
- [6] Moudgil R K, Ahluwalia P K and Pathak K N 1997 *Phys. Rev. B* **56** 14 776  
Gold A 1993 *Z. Phys. B* **90** 361
- [7] Gold A 1992 *Z. Phys. B* **89** 213
- [8] Jerome D 1991 *Science* **252** 1509
- [9] For a theoretical review, see  
Li Q P and Das Sarma S 1991 *Phys. Rev. B* **43** 11 768  
Calmels L and Gold A 1995 *Phys. Rev. B* **52** 10 841  
Das Sarma S and Hwang E H 1996 *Phys. Rev. B* **54** 1936
- [10] For review of experimental study, see  
Hansen W 1991 *Quantum Coherence in Mesoscopic Systems* ed B Kramer (New York: Plenum) p 23
- [11] Gold A and Ghazali A 1990 *Phys. Rev. B* **41** 7626
- [12] Singwi K S, Tosi M P, Land R H and Sjölander A 1968 *Phys. Rev.* **176** 589  
Singwi K S and Tosi M P 1981 *Solid State Physics* vol 36 (New York: Academic) p 177
- [13] Caparica A A and Hipolito O 1982 *Phys. Rev. A* **26** 2832
- [14] Calmels L and Gold A 1995 *Phys. Rev. B* **51** 8426